Letter

Numerical case for identifying paired quantum Hall phases by their daughter states

Misha Yutushui [1,*] Arjun Dey [2,3,*] and David F. Mross [1]

[1]*Department of Condensed Matter Physics, Weizmann Institute of Science, Rehovot 7610001, Israel*

[2]*Laboratory for Theoretical and Computational Physics, PSI Center for Scientific Computing, Theory and Data, 5232 Villigen PSI, Switzerland*

[3]*Institute of Physics, École Polytechnique Fédérale de Lausanne (EPFL), 1015 Lausanne, Switzerland*

(Received 9 September 2025; accepted 4 February 2026; published 30 April 2026)

Many candidate non-Abelian quantum Hall states are accompanied by nearby "daughter" states, which are proposed to identify their topological order. Combining exact diagonalization and trial wave functions, we provide numerical evidence that daughter states reliably predict the parent topological phase. In the context of bilayer graphene and wide GaAs quantum wells, we show that the same interactions simultaneously stabilize Pfaffian, anti-Pfaffian, and their daughters, while suppressing the Jain states. The competition between Pfaffian and anti-Pfaffian, which is decided by particle-hole symmetry-breaking interactions, can likewise be deduced from their daughters. These findings strongly support the daughter-state-based identification of non-Abelian quantum Hall phases.

DOI: 10.1103/g4nc-cpcr

Introduction. Non-Abelian particles are highly sought for their exotic properties [1,2]. Their many-body wave function encodes a quantum state together with its topological history [3–6]. As a result, controlled braiding of non-Abelian anyons could allow for intrinsically fault-tolerant manipulation of quantum information [7,8]. Fractional quantum Hall states [9–11] at specific filling factors are currently the leading platforms for realizing these particles. The simplest among them are Ising anyons, which are expected to occur in a half-filled Landau level of electrons [12–15]. Half-filled plateaus have been observed in various platforms, including GaAs heterostructures [16–19], mono- and multilayers of graphene [20–25], and other materials [26,27].

The experimental identification of non-Abelian quantum Hall states represents a significant challenge. It requires sensitivity to neutral modes that do not directly respond to conventional probes [28–33]. While various experimental protocols have been proposed to determine topological order [34–38], their implementation remains challenging or inconclusive [39–44]. Alternatively, multiple recent experiments have used Levin-Halperin daughter states [45] as indicators for the topological order at even-denominator states [46–48]. These daughter states arise when pairs of composite fermions form a bosonic integer quantum Hall state [49,50]. Under the assumption that the pairing is the same as in the parent even-denominator state, the daughter-state filling factors can uniquely determine the parent topological order.

The validity of this assumption has not been tested experimentally or numerically. Moreover, daughter-state filling factors coincide with those of the ubiquitous Jain states at $\nu = \frac{n}{2n+1}$, and the topological order of the observed plateaus has not been established. They have been identified as daughter states by being anomalously strong and violating the monotonic decay of the Jain-state gap with $|n|$ [51,52].

In this Letter, we construct trial wave functions and use exact diagonalization techniques to test the relationship between even-denominator states, their daughters, and the Jain states. For two families of Hamiltonians, we find that the strengths of parents and daughters are well correlated, indicating their common origin. Moreover, they exhibit a very similar competition against states of unpaired composite fermions, i.e., the composite Fermi liquid and the Jain states. Finally, we find that particle-hole symmetry-breaking interactions [53–58], which lift the degeneracy between Pfaffian and anti-Pfaffian, enhance or suppress the parent topological orders and their specific daughters simultaneously.

Trial wave functions. As the primary diagnostic of quantum Hall states, we use the overlap between the ground state of a microscopic Hamiltonian and parameter-free model wave functions. For paired states and Jain states, trial wave functions based on the composite-fermion or parton paradigms are well established [3,4,52,59–61]. The daughter states at $\nu = \frac{6}{11}$ and $\frac{6}{13}$ have integer shifts $\mathcal{S} = 6$ and -2, respectively, and admit the parton representations [49,62]

$$\Phi_{\frac{6}{11}} = P_{\mathrm{LLL}}[\phi_3\phi_2\phi_1], \quad \Phi_{\frac{6}{13}} = P_{\mathrm{LLL}}\left[\phi_3^*\phi_2^*\phi_1^3\right], \qquad (1)$$

where P_{LLL} is the lowest Landau projection and ϕ_n is the wave function of n filled Landau levels.

The other pertinent daughter states do not permit wave functions of this type due to a fractional *shift* $\mathcal{S}$ [63]. States at $\nu = \frac{5}{11}$ and $\frac{7}{13}$ can be obtained by applying a particle-hole

*These authors contributed equally to this work.

Published by the American Physical Society under the terms of the Creative Commons Attribution 4.0 International license. Further distribution of this work must maintain attribution to the author(s) and the published article's title, journal citation, and DOI.

transformation to the wave functions in Eq. (1). For $\nu = \frac{9}{17}$ and the $\nu = \frac{9}{19}$ daughter of the $\mathrm{SU}(2)_2$, this option is not available, and we employ the anyon condensation approach [64,65]. Specifically, for the $\nu = \frac{9}{17}$ daughter, we place *pairs* of the quasiholes of a $\nu = 1$ integer state into a bosonic $\nu = \frac{2}{9}$ Jain state $\Phi_{\frac{2}{9}} = \phi_1^5 \phi_2^*$, resulting in the wave function

$$\Phi_{\frac{9}{17}}(z) = \phi_1(z) \int_{u_a} \prod_i^{N_e} \prod_a^{N_q} (z_i - u_a)^2 \Phi^*_{\frac{2}{9}}(u_a). \tag{2}$$

The integral is nonzero for $N_q = \frac{2}{9}(2N_e + 3)$ quasihole pairs, correctly reproducing the quantum numbers of the $\nu = \frac{9}{17}$ daughter state. For the $\nu = \frac{9}{19}$ daughter, we replace the integer state by a $\nu = \frac{1}{3}$ Laughlin state $\phi_1 \to \phi_1^3$ and complex conjugate the integral. We further multiply the wave function by $\prod_{i<j} |z_i - z_j|^2$, which improves numerical convergence without affecting the topological phase.

The resulting phases are Abelian topological orders described by a charge vector $q = (1, 0, 0)$ and K-matrices

$$K_{\frac{9}{17}} = \begin{pmatrix} 1 & -2 & -2 \\ -2 & -4 & -5 \\ -2 & -5 & -4 \end{pmatrix}, \quad K_{\frac{9}{19}} = \begin{pmatrix} 3 & -2 & -2 \\ -2 & 4 & 5 \\ -2 & 5 & 4 \end{pmatrix}. \tag{3}$$

Both matrices have two positive and one negative eigenvalues, implying a thermal Hall conductance of $\kappa_{xy} = 1$ (in units of $\frac{\pi^2 k_B^2}{3h} T$), consistent with daughter states but not with Jain states at those fillings. Finally, using the spin vectors $s_{9/17} = (\frac{1}{2}, 1, 2)$ and $s_{9/19} = (\frac{3}{2}, 1, 2)$ to compute the shifts as $\mathcal{S} = \frac{2}{\nu} \boldsymbol{s} K^{-1} \boldsymbol{q}$, we obtain the expected values for the daughter states, i.e., $-\frac{1}{3}$ and $\frac{13}{3}$ [49].

We obtain second-quantized representations of the wave functions in Eqs. (1) and (2) by computing their overlaps with a full set of basis states in the corresponding Hilbert space via Monte Carlo sampling; see Appendix A: Monte Carlo for anyon condensation states for details. Similarly, we construct the $\nu = \frac{2}{5}, \frac{3}{7}$ Jain states and the $\mathrm{SU}(2)_2$ parton states. For the $\nu = \frac{1}{3}$ state and the Pfaffian, we use Jack polynomials [66].

Daughter states in GaAs and graphene. We consider Coulomb interactions projected into one partially filled Landau level of single-electron orbitals of the form $\Psi(\theta) = (\psi_0 \cos\theta, \psi_1 \sin\theta)$. Here, ψ_n are the wave functions of nonrelativistic free electrons in the nth Landau level. In particular, the cases $\theta = 0$ and $\theta = \frac{\pi}{2}$ describe the lowest and first excited Landau levels of GaAs. Previous numerical studies [12–15,53–58] found that Coulomb interactions in the half-filled lowest Landau level favor a composite Fermi liquid and Pfaffian or anti-Pfaffian pairing in the first excited Landau level.

In bilayer graphene, the eightfold degenerate zeroth Landau level contains four $\theta = 0$ levels and four with an intermediate θ that depends weakly on the magnetic field and displacement field. The values range between $\theta_{12\,\mathrm{T}} \approx 0.41\pi$ at $B = 12\,\mathrm{T}$ and $\theta_{31\,\mathrm{T}} \approx 0.36\pi$ at $B = 31\,\mathrm{T}$ under typical experimental conditions [67,68]; see Appendix B: Haldane pseudopotentials for bilayer graphene.

We use the DiagHam library [69] to exactly diagonalize $H(\theta)$ in a spherical geometry. For $N_e = 20$ particles and $N_\phi = 37$ magnetic flux quanta, a compressible composite Fermi liquid and an incompressible state with Pfaffian pairing can both be realized. Figure 1 shows that the ground-state transitions from a composite Fermi liquid at $\theta \lesssim 0.37\pi$ to a paired state, with the largest overlap for $\theta \approx \theta_{12\,\mathrm{T}}$. The $\nu = \frac{7}{13}$ daughter of the Moore-Read Pfaffian occurs for $N_e = 17$, $N_\phi = 28$. As its trial state, we use the particle-hole conjugate of the $\nu = \frac{6}{13}$ daughter state defined in Eq. (1). We find that its overlap with the $H(\theta)$ ground state also exhibits a pronounced maximum near θ_{12T}. The overlap at $\theta \approx 0$ is significant, which we attribute to the absence of a strong competitor; i.e., the daughter state at this particle number is not aliased with (does not reside in the same Hilbert space as) any Jain state (see Appendix C: Daughter-state Hilbert spaces and aliasing).

The $\nu = \frac{8}{17}$ daughter of the Pfaffian is the particle-hole conjugate of $\Psi_{\frac{9}{17}}$ in Eq. (2), and both $\Psi_{\frac{8}{17}}, \Psi_{\frac{9}{17}}$ can occur in the $N_e = 12$, $N_\phi = 23$ system; i.e., the Pfaffian daughter is aliased with its own particle-hole conjugate. The eigenstates of any two-body Hamiltonian in this system have a well-defined transformation under particle-hole transformation, which is even for the $H(\theta)$ ground state. Consequently, we compare it to the equal superposition of our $\nu = \frac{8}{17}$ and $\nu = \frac{9}{17}$ trial states. The resulting overlap in Fig. 1 closely tracks the ground-state overlap of the Pfaffian.

To test whether this behavior is indeed related to the specific pairing channel, we repeat this analysis for the $\mathrm{SU}(2)_2$ state and its two daughters. We find that all of these states are strongly suppressed as θ increases. These results support the hypothesis that the experimental observations of $\nu = \frac{7}{13}$ and $\nu = \frac{8}{17}$ daughter states (or their particle-hole conjugates) point to the Pfaffian (or anti-Pfaffian) topological order at half-filling.

Daughter states in wide quantum wells. In wide GaAs quantum wells, the transverse extent w of the well represents a continuous tuning parameter. A nonzero width reduces the energetic penalty for electrons at small in-plane separation and can promote pairing at even-denominator fillings of the lowest Landau level. In practice, an in-plane magnetic field or tuning the electron density with respect to the transverse subbands permits *in situ* control over w.

To model the wide quantum well, we replace the Coulomb interactions by $V_w(r) = \frac{1}{\sqrt{r^2 + w^2}}$ [70]. As before, we numerically obtain the ground states on a sphere for different choices of (N_e, N_ϕ) and compute the overlaps with the same trial states. The results are shown in the right panel of Fig. 1. With increasing w, the composite Fermi liquid is suppressed, while the Pfaffian order and its two daughters are favored, consistent with the experimental observations of Ref. [46]. The f-wave paired state and its two daughters are not favorable at any w.

Competition between Jain and daughter states. The results presented above support the assertion that the presence of specific daughter states points to the parent topological order. We thus turn to the question of whether the observed plateaus in bilayer graphene and wide quantum wells are indeed daughter states or merely Jain states. To address this issue numerically, we assess the strengths of different topological phases as θ or w are varied. Specifically, for any $L = 0$ ground state, we compute the gap Δ to the first excited state in the same Hilbert

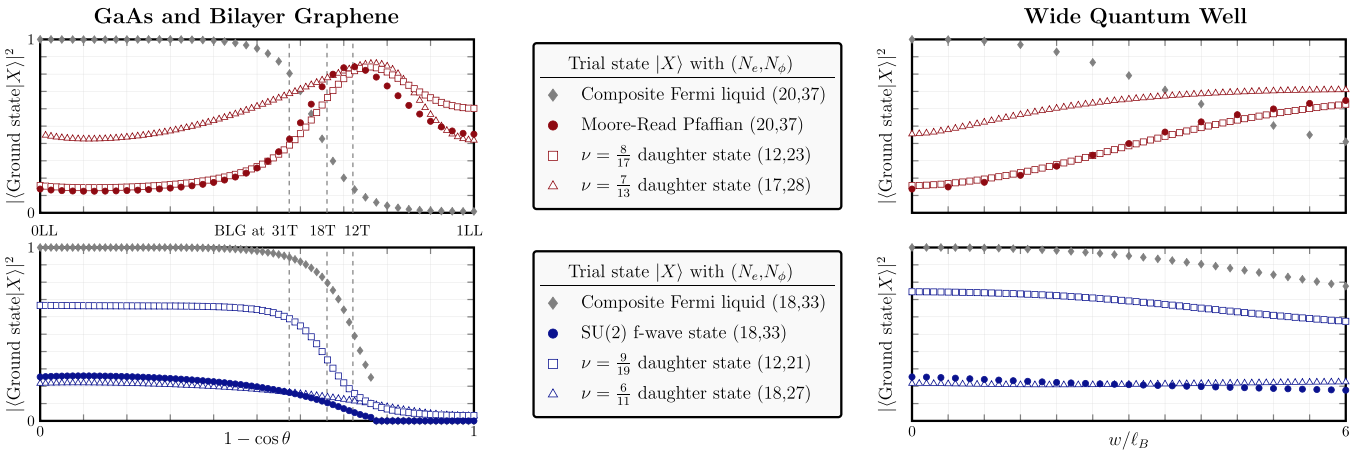


FIG. 1. Paired states and their daughters in graphene and GaAs. Left panel: The two lowest orbital Landau-level wave functions of GaAs and bilayer graphene can be parametrized as $\Psi = (\psi_0 \cos\theta, \psi_1 \sin\theta)$ for different choices of θ. When the parameter $\theta \approx 0$, Coulomb interactions favor a composite Fermi liquid at $\nu = \frac{1}{2}$. For $\theta \approx \frac{\pi}{2}$, we instead find that the Pfaffian or anti-Pfaffian states and their daughters are favored. In contrast, f-wave pairing and the corresponding daughters are not favorable for any θ. Right panel: For interactions modeling a wide quantum well, we again find that the Pfaffian state and its daughters become simultaneously favorable with increasing width w, while the composite Fermi liquid is suppressed. States with f-wave pairing or its daughters are never favored.

space, focusing on systems where Jain states, paired states, and daughter states do not directly compete. Unfortunately, an extrapolation of the gaps to the thermodynamic limit is not possible due to the small number of accessible system sizes. To increase the system size at filling $\nu = \frac{q}{p}$, one needs to increment $(N_e, N_\phi) \to (N_e + q, N_\phi + p)$—a vast increase in Hilbert space size at daughter state fillings (cf. Appendix C: Daughter-state Hilbert spaces and aliasing for Hilbert space dimensions). Moreover, all daughter states apart from the one at $\nu = \frac{7}{13}$ (and its particle-hole conjugate) are aliased with Jain states at available system sizes. We thus restrict our study of gaps to the $\nu = \frac{7}{13}$ daughter, the first three Jain states, and the Pfaffian.

Figure 2 shows the numerically obtained gap whenever the ground state has zero angular momentum. As expected, we find that all Jain states are suppressed with increasing θ or w, and higher-order Jain states are affected more strongly [71]. In contrast, the $\nu = \frac{7}{13}$ state and Pfaffian are strengthened at intermediate values and can become favored even over low-order Jain states. These findings support the claim that a well-developed quantum Hall state at $\frac{6}{13}$ (or $\frac{7}{13}$) with much weaker or absent states at lower Jain fillings, such as $\frac{5}{11}$, $\frac{4}{9}$ (or $\frac{6}{11}$, $\frac{5}{9}$), is likely to be a daughter state.

Landau-level mixing. All results presented so far were obtained for models with pure two-body interactions in a single Landau level. For such interactions, any quantum Hall state at filling factor ν is degenerate with its hole conjugate at filling $1 - \nu$. At half-filling, different pairing channels such as the Pfaffian and anti-Pfaffian orders are of identical strength and must likewise be degenerate.

In experiments, particle-hole symmetry is broken due to Landau-level mixing. When the mixing is weak, it can be included perturbatively through a modified interaction between electrons in a single Landau level. At the leading order, Landau-level mixing renormalizes the two-body interactions, which preserve particle-hole symmetry, and introduces three-body interactions, which break it. Numerous studies used such interactions to assess the competition between Pfaffian and anti-Pfaffian in GaAs at $\nu = \frac{5}{2}$ [72]. Instead of revisiting this debate, we focus on the most pertinent question in the present context: Is the realization of Pfaffian daughters instead of anti-Pfaffian daughters indicative of the topological order at half-filling?

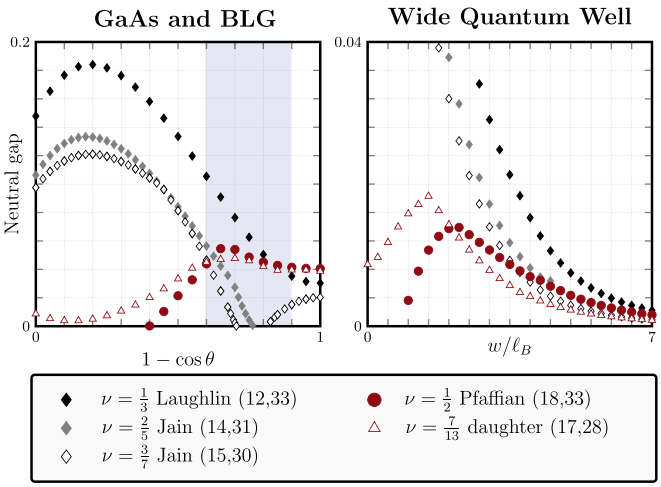


FIG. 2. Competition between Jain states and daughter states. We numerically compute the lowest-energy eigenstates for systems whose (N_e, N_ϕ) match the indicated states. When the ground state has angular momentum zero, we compute the energy difference to the first excited states. As anticipated, we find that this neutral gap is suppressed more quickly with θ or w for higher-order Jain states, such that the daughter state becomes competitive. The shaded region in the left plot indicates where Ref. [73] found an $L = 0$ ground state in an $(N_e, N_\phi) = (20, 40)$ system, which corresponds to the $\frac{8}{17}$ daughter and is consistent with our findings.

TABLE I. Pseudopotentials. Antisymmetrizing a pure three-body Hamiltonian with respect to particle-hole leads to two-body pseudopotentials whose strength depends (weakly) on the number N_ϕ of magnetic flux quanta piercing the sphere.

	$\mathcal{P}_{ijk}(3) - \bar{\mathcal{P}}_{ijk}(3)$		$\mathcal{P}_{ijk}(3) - \bar{\mathcal{P}}_{ijk}(3)$		
N_ϕ	$V_1^{(2)}$	$V_3^{(2)}$	$V_1^{(2)}$	$V_3^{(2)}$	$V_5^{(2)}$
23	−1.612 40	−0.571 75	−1.107 20	−0.306 08	−0.746 66
25	−1.618 54	−0.570 92	−1.120 06	−0.303 89	−0.742 48
28	−1.626 07	−0.569 92	−1.135 86	−0.301 25	−0.737 53

As a first test, we use the well-known parent Hamiltonian of the Pfaffian, $H_3 = \sum_{i<j<k} \mathcal{P}_{ijk}(3)$, where $\mathcal{P}_{ijk}(\ell)$ projects the electron triplet i, j, k onto a state with relative angular momentum ℓ. These interactions have particle-hole symmetric contributions, which are expressible by two-body pseudopotentials [74–77] and antisymmetric components. Using the H_3 at the shift of the $\nu = \frac{7}{13}$ daughter state, we find ≈84% squared overlap of the $N_\phi = 27$ ground state with the Pfaffian daughter trial wave function. In contrast, the $\nu = \frac{6}{13}$ ground state exhibits an overlap below 1% with the anti-Pfaffian daughter.

Encouraged by this finding, we systematically perturb the particle-hole symmetric Hamiltonian $H(\theta)$ studied above by a particle-hole *antisymmetric* interaction

$$\delta H_\ell \equiv \sum_{i<j<k} [\mathcal{P}_{ijk}(\ell) - \bar{\mathcal{P}}_{ijk}(\ell)]. \tag{4}$$

For $\ell = 3$ or 5, the resulting δH_ℓ includes not only the three-body potential, but also the first and third (and fifth) two-body pseudopotentials, whose strengths depend on the number of magnetic flux quanta piercing the sphere (see Table I). We then determine ground-state overlaps and the many-body gap of $H_{\text{total}} = H(\theta_{18T}) + \gamma \delta H$, where $\gamma = 0$ realizes the Pfaffian or its daughters according to Fig. 1.

When we perturb with δH_3, the many-body gap at the Pfaffian shift $(N_e, N_\phi) = (14, 25)$ increases as expected for positive γ, as shown in Fig. 3 (left). Simultaneously, the overlap with the Pfaffian wave function increases (see Fig. 3, right). For the system size $(N_e, N_\phi) = (17, 28)$, appropriate for the $\frac{7}{13}$ daughter state, we observe a very similar evolution of the gap and overlap, i.e., an increase for positive γ. We do not show the gap of the second Pfaffian daughter at $\nu = \frac{8}{17}$, since it is aliased with its own particle-hole conjugate at the only accessible system size. Still, the overlap with the trial state follows the same trend as for the other two states. When perturbing with δH_5, we find that a positive coefficient suppresses gaps and overlaps for the Pfaffian and its two daughters.

The gaps and overlaps for anti-Pfaffian and its two daughters behave exactly oppositely; they correspond to $\gamma \to -\gamma$ and are not shown separately. We interpret these results as evidence that the observation of daughter states can indeed distinguish between parent Pfaffian and anti-Pfaffian orders, independently of the precise particle-hole symmetry-breaking perturbation.

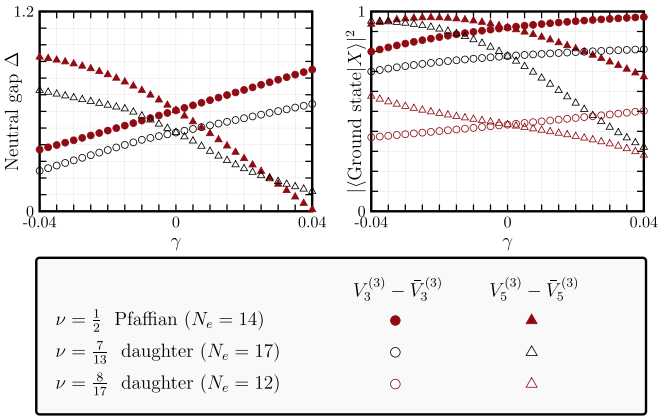


FIG. 3. Particle-hole symmetry breaking. We study Landau-level mixing by perturbing the $\theta = \theta_{18T}$ Coulomb Hamiltonian with the particle-hole antisymmetric part of the third and fifth three-body pseudopotentials. The neutral gaps Δ (left) and the ground-state overlaps (right) of the Pfaffian and its $\nu = \frac{6}{13}$ daughter closely track one another for both perturbations. For $\nu = \frac{8}{17}$, we only show the overlap but no gap, since this state is aliased with its own particle-hole conjugate in the only available system, for which $N_e = 12$.

Conclusions. We have provided numerical evidence that the quantum Hall plateaus flanking half-filled states in bilayer graphene and wide GaAs quantum wells are Levin-Halperin daughter states. More generally, our study supports the case that the topological orders of paired quantum Hall states can be inferred from their daughters, including the distinction between Pfaffian and anti-Pfaffian. We find no indication of different pairing channels at half-filling in the zeroth Landau level of bilayer graphene and GaAs. Still, quantum Hall states with other pairing channels could also be diagnosed by their daughters; see Appendix D: F-wave paired states and their daughters for a specific example, where two-body interactions stabilizing the $SU(2)_2$ topological order also favor its daughters.

Acknowledgments. It is a pleasure to acknowledge illuminating discussions with Ajit Balram, Maria Hermanns, and Yuval Ronen. This work was supported by the Israel Science Foundation (ISF) under Grant No. 2572/21 and by the Minerva Foundation with funding from the Federal German Ministry for Education and Research. A.D. thanks the High Performance Computing and Emerging Technologies group at PSI, which maintains the Merlin7 cluster, where part of the numerical work was done.

Data availability. The data that support the findings of this article are available in the Zenodo repository [78].

Appendix A: Monte Carlo for anyon condensation states. To obtain a Fock-space representation of a real-space wave function such as Eq. (2), we evaluate a large number of multi-dimensional integrals of the form

$$\begin{aligned}\langle \Phi_I | \Psi_{\text{trial}} \rangle &= \int_z \Phi_I(z^*) \Psi_{\text{trial}}(z) \\ &= \int_z \Phi_I(z^*) \Psi(z) \int_u (u - z)^k \Psi_{\text{QP}}(u^*),\end{aligned} \tag{A1}$$

with integer k. Here, the N-component vector $I = (i_1, i_2, \ldots, i_N)$ defines a basis state of the Fock space; in

the spherical geometry,

$$\Phi_I = \det \begin{pmatrix} Y^Q_{Q,m_{i_1}}(\boldsymbol{r}_1) & Y^Q_{Q,m_{i_1}}(\boldsymbol{r}_2) & \dots \\ Y^Q_{Q,m_{i_2}}(\boldsymbol{r}_1) & Y^Q_{Q,m_{i_2}}(\boldsymbol{r}_2) & \dots \\ \vdots & \vdots & \ddots \end{pmatrix}, \tag{A2}$$

where $Y^Q_{l,m}$ are monopole harmonics. The number of basis states grows exponentially with the system size, and evaluating all these Slater determinants is the numerical bottleneck. However, we note that changing the u coordinate in Eq. (A1) affects Ψ_{trial} but not Φ_I; i.e., all the determinants can be reused for sampling the overlap. To reduce the computational cost, we thus make 10^3–10^4 u updates in between z updates.

To refine the wave functions obtained via Monte Carlo sampling, we then project them onto the $\boldsymbol{L}^2 = 0$ subspace as done in Ref. [79]. By comparing the final wave functions resulting from independent runs with comparable numerical effort, we estimate that the squared overlaps of the numerically obtained wave functions with the exact ones exceed 99%.

Appendix B: Haldane pseudopotentials for bilayer graphene. The zeroth Landau level of bilayer graphene contains four $N = 0$ and four $N = 1$ orbitals that are describable by two-component wave functions $\Psi = (\psi_0 \cos\theta, \psi_1 \sin\theta)$ with zero and nonzero θ, respectively. In spherical geometry, the nth Landau level has $2(Q + n) + 1$ states, where Q is the monopole strength. To have equal degeneracies for both $n = 0$ and $n = 1$ components, we thus use the monopole strengths $Q_n = Q - n$.

The orbitals in the zeroth Landau level of bilayer graphene are thus

$$\mathcal{Y}^Q_m = \left(C_0 Y^Q_{Q,m}, C_1 Y^{Q-1}_{Q,m}\right), \tag{B1}$$

where we introduced the vector $(C_0, C_1) = (\cos\theta, \sin\theta)$. The matrix elements of a real-space density-density potential $V(r)$ are then computed as

$$\begin{aligned} \mathcal{V}^{m_3,m_4}_{m_1,m_2}(\theta) &= \int_{\boldsymbol{r}_1}\int_{\boldsymbol{r}_2} V(|\boldsymbol{r}_1 - \boldsymbol{r}_2|) \\ &\quad \times \left(\mathcal{Y}^{Q\dagger}_{m_1}(\boldsymbol{r}_1)\cdot \mathcal{Y}^Q_{m_3}(\boldsymbol{r}_1)\right)\left(\mathcal{Y}^{Q\dagger}_{m_2}(\boldsymbol{r}_2)\cdot \mathcal{Y}^Q_{m_4}(\boldsymbol{r}_2)\right) \\ &= \sum_{i=0,1}\sum_{j=0,1} [C_i C_j]^2 V^{m_3,m_4}_{m_1,m_2}(Q_i, Q_j). \end{aligned} \tag{B2}$$

In the last row, we used the nonrelativistic matrix elements for electrons in two different ith and jth Landau levels with monopole strengths Q_i and Q_j, respectively, i.e.,

$$\begin{aligned} V^{m_3,m_4}_{m_1,m_2}(Q; Q_i, Q_j) &= \int_{\boldsymbol{r}_1}\int_{\boldsymbol{r}_2} V(|\boldsymbol{r}_1 - \boldsymbol{r}_2|) \\ &\quad \times Y^{Q_i *}_{Q,m_1}(\boldsymbol{r}_1) Y^{Q_i}_{Q,m_3}(\boldsymbol{r}_1)\, Y^{Q_j *}_{Q,m_2}(\boldsymbol{r}_2) Y^{Q_j}_{Q,m_4}(\boldsymbol{r}_2). \end{aligned} \tag{B3}$$

Here, the number of states is Q, the same for both the ith and jth Landau levels. Equation (B2) involves these elements for $i, j = 0, 1$ Landau-level indices.

For a rotationally symmetric potential, only matrix elements with $\Delta m = m_3 - m_1 = m_4 - m_2$ are nonzero. Expanding the real-space potentials in terms of Legendre polynomials $V(\theta) = \sum_k V_k P_k(\cos(\theta))$, using the addition theorem of spherical harmonics and the integral of three monopole harmonics [52,80–82], the matrix elements are readily found to be

$$\begin{aligned} V^{m_3,m_4}_{m_1,m_2}(Q; Q_i, Q_j) &= \sum_{k=0}^{2Q} V_k (2Q+1)^2 (-1)^{2Q-m_3-m_2} \\ &\quad \times \begin{pmatrix} Q & k & Q \\ m_1 & \Delta m & -m_3 \end{pmatrix}\begin{pmatrix} Q & k & Q \\ -Q_i & 0 & Q_i \end{pmatrix} \\ &\quad \times \begin{pmatrix} Q & k & Q \\ m_2 & \Delta m & -m_4 \end{pmatrix}\begin{pmatrix} Q & k & Q \\ -Q_j & 0 & Q_j \end{pmatrix}. \end{aligned} \tag{B4}$$

The Haldane pseudopotentials corresponding to $V^{m_3,m_4}_{m_1,m_2}(Q; Q_i, Q_j)$ are given by

$$\begin{aligned} H^Q_L(Q_i, Q_j) &= \sum_{m_i=-Q}^{Q} V^{m_3,m_4}_{m_1,m_2}(Q; Q_i, Q_j) \\ &\quad \times \sum_{M'} \langle 2Q - L, M' | Q, m_3; Q, m_4\rangle \\ &\quad \times \langle Q, m_1; Q, m_2 | 2Q - L, M'\rangle, \end{aligned} \tag{B5}$$

$$\begin{aligned} &= (2Q+1)^2 (-1)^{2Q-Q_i-Q_j-L} \\ &\quad \times \sum_{k=0}^{2Q} V_k \begin{pmatrix} Q & k & Q \\ -Q_i & 0 & Q_i \end{pmatrix}\begin{pmatrix} Q & k & Q \\ -Q_j & 0 & Q_j \end{pmatrix} \\ &\quad \times \begin{Bmatrix} 2Q - L & Q & Q \\ k & Q & Q \end{Bmatrix}. \end{aligned} \tag{B6}$$

Finally, we obtain the bilayer graphene pseudopotentials as

$$\mathcal{H}^\theta_L = \sum_{i=0,1}\sum_{j=0,1} [C_i C_j]^2 H^Q_L(Q_i, Q_j). \tag{B7}$$

TABLE II. Finite-size Hilbert spaces of daughter states. The filling factor ν and shift $\mathcal{S}$ determine the required number of flux quanta N_ϕ piercing the surface sphere for N_e electrons. Here, we list the dimensions of these Hilbert spaces and indicate when the Hilbert spaces coincide with those of other daughter states, Jain states, or paired quantum Hall states. Systems listed in gray are included for completeness, but were not part of this study.

ν	$\mathcal{S}$	N_e	N_ϕ	$D_{L_z=0}$	$D_{\boldsymbol{L}=0}$	Aliased states
$\frac{8}{17}$	$\frac{5}{2}$	12	23	61 108	127	$\nu = \frac{3}{7}$ Jain, PH-Pfaffian, $\nu = \frac{9}{17}$ daughter
		20	40	2.8×10^9	903 256	$\nu = \frac{10}{19}$ daughter
$\frac{7}{13}$	$\frac{25}{7}$	17	28	901 723	902	
		24	41	3.5×10^9	1099 354	$\frac{3}{5}$ Jain, $\nu = \frac{1}{2}$ with $\ell = 5$ pairing
$\frac{9}{19}$	$\frac{13}{3}$	12	21	16 660	58	$\nu = \frac{3}{5}$ Jain, $\frac{4}{9}$ Jain, Pfaffian
		21	40	2.8×10^9	903 256	$\nu = \frac{9}{17}$ daughter
$\frac{6}{11}$	6	18	27	246 448	319	$\nu = \frac{2}{3}$ Jain, $\nu = \frac{1}{2}$ with $\ell = 7$ pairing
		24	38	2.9×10^8	114 049	

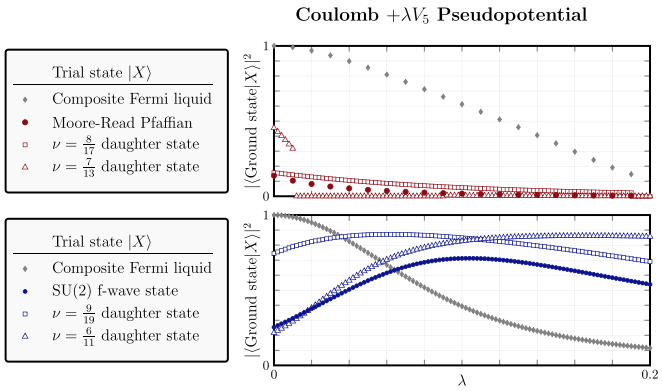


FIG. 4. $SU(2)_2$ and its daughters for strong V_5 pseudopotential. Perturbing Coulomb interactions in the lowest Landau level via the fifth Haldane pseudopotential suppresses the composite Fermi liquid at $\nu = \frac{1}{2}$. It simultaneously favors the f-wave paired state and its two daughters. In contrast, the Pfaffian or anti-Pfaffian and their daughters are not favored. The sharp features in the top plot correspond to crossings between levels with different angular momentum.

Appendix C: Daughter-state Hilbert spaces and aliasing. On a finite sphere, the particle number and flux required to realize a particular topological order in the ground state are determined by the filling factor and shift according to

$$N_\phi = \nu^{-1} N_e - \mathcal{S}. \tag{C1}$$

Table II summarizes the Hilbert spaces and their dimensions for the four daughter states. Black rows indicate the systems studied in this work, while gray rows indicates the next systems where the same orders could occur. The final column lists other states that can also be realized in the same Hilbert space.

Appendix D: F-wave paired states and their daughters. At present, there is no strong candidate for an experimentally realized $SU(2)_2$ topological order. Numerical works have suggested such a state in monolayer graphene at [23,83], but found it to be rather fragile. Its stabilization requires a strong fifth Haldane pseudopotential, V_5 [81], which is not realized in low Landau levels where most half-filled states occur. Still, we test the generality of the daughter-state-based identification by studying a Coulomb Hamiltonian perturbed by V_5.

The wave function overlaps presented in Fig. 4 show that the ground state of the half-filled Landau level evolves from a composite Fermi liquid to the $SU(2)_2$ order at moderate V_5. Simultaneously, the two daughter states of this order also become favorable. In contrast, neither the Pfaffian order nor its daughters are stabilized by these interactions.

[1] C. Nayak, S. H. Simon, A. Stern, M. Freedman, and S. Das Sarma, Non-Abelian anyons and topological quantum computation, Rev. Mod. Phys. **80**, 1083 (2008).

[2] A. Stern, Non-Abelian states of matter, Nature (London) **464**, 187 (2010).

[3] J. K. Jain, Incompressible quantum Hall states, Phys. Rev. B **40**, 8079 (1989).

[4] G. Moore and N. Read, Non-Abelions in the fractional quantum Hall effect, Nucl. Phys. B **360**, 362 (1991).

[5] X. G. Wen, Non-Abelian statistics in the fractional quantum Hall states, Phys. Rev. Lett. **66**, 802 (1991).

[6] N. Read and E. Rezayi, Beyond paired quantum Hall states: Parafermions and incompressible states in the first excited Landau level, Phys. Rev. B **59**, 8084 (1999).

[7] M. Freedman, M. Larsen, and Z. Wang, A modular functor which is universal for quantum computation, Commun. Math. Phys. **227**, 605 (2002).

[8] L. Hormozi, G. Zikos, N. E. Bonesteel, and S. H. Simon, Topological quantum compiling, Phys. Rev. B **75**, 165310 (2007).

[9] D. C. Tsui, H. L. Stormer, and A. C. Gossard, Two-dimensional magnetotransport in the extreme quantum limit, Phys. Rev. Lett. **48**, 1559 (1982).

[10] R. B. Laughlin, Anomalous quantum Hall effect: An incompressible quantum fluid with fractionally charged excitations, Phys. Rev. Lett. **50**, 1395 (1983).

[11] F. D. M. Haldane, Fractional quantization of the Hall effect: A hierarchy of incompressible quantum fluid states, Phys. Rev. Lett. **51**, 605 (1983).

[12] R. H. Morf, Transition from quantum Hall to compressible states in the second Landau level: New light on the $\nu = 5/2$ enigma, Phys. Rev. Lett. **80**, 1505 (1998).

[13] K. Park, V. Melik-Alaverdian, N. E. Bonesteel, and J. K. Jain, Possibility of p-wave pairing of composite fermions at $\nu = \frac{1}{2}$, Phys. Rev. B **58**, R10167 (1998).

[14] E. H. Rezayi and F. D. M. Haldane, Incompressible paired Hall state, stripe order, and the composite fermion liquid phase in half-filled Landau levels, Phys. Rev. Lett. **84**, 4685 (2000).

[15] V. W. Scarola, K. Park, and J. K. Jain, Cooper instability of composite fermions, Nature (London) **406**, 863 (2000).

[16] R. Willett, J. P. Eisenstein, H. L. Störmer, D. C. Tsui, A. C. Gossard, and J. H. English, Observation of an even-denominator quantum number in the fractional quantum Hall effect, Phys. Rev. Lett. **59**, 1776 (1987).

[17] J. P. Eisenstein, R. Willett, H. L. Stormer, D. C. Tsui, A. C. Gossard, and J. H. English, Collapse of the even-denominator fractional quantum Hall effect in tilted fields, Phys. Rev. Lett. **61**, 997 (1988).

[18] Y. W. Suen, L. W. Engel, M. B. Santos, M. Shayegan, and D. C. Tsui, Observation of a $\nu = 1/2$ fractional quantum Hall state in a double-layer electron system, Phys. Rev. Lett. **68**, 1379 (1992).

[19] C. Wang, A. Gupta, S. K. Singh, Y. J. Chung, L. N. Pfeiffer, K. W. West, K. W. Baldwin, R. Winkler, and M. Shayegan, Even-denominator fractional quantum Hall state at filling factor $\nu = 3/4$, Phys. Rev. Lett. **129**, 156801 (2022).

[20] D. K. Ki, V. I. Fal'ko, D. A. Abanin, and A. F. Morpurgo, Observation of even denominator fractional quantum Hall effect in suspended bilayer graphene, Nano Lett. **14**, 2135 (2014).

[21] Y. Kim, D. S. Lee, S. Jung, V. Skákalová, T. Taniguchi, K. Watanabe, J. S. Kim, and J. H. Smet, Fractional quantum Hall states in bilayer graphene probed by transconductance fluctuations, Nano Lett. **15**, 7445 (2015).

[22] A. A. Zibrov, E. M. Spanton, H. Zhou, C. Kometter, T. Taniguchi, K. Watanabe, and A. F. Young, Even-denominator

fractional quantum Hall states at an isospin transition in monolayer graphene, Nat. Phys. **14**, 930 (2018).
[23] Y. Kim, A. C. Balram, T. Taniguchi, K. Watanabe, J. K. Jain, and J. H. Smet, Even-denominator fractional quantum Hall states in higher Landau levels of graphene, Nat. Phys. **15**, 154 (2019).
[24] Y. Chen, Y. Huang, Q. Li, B. Tong, G. Kuang, C. Xi, K. Watanabe, T. Taniguchi, G. Liu, Z. Zhu, L. Lu, F.-C. Zhang, Y.-H. Wu, and L. Wang, Tunable even- and odd-denominator fractional quantum Hall states in trilayer graphene, Nat. Commun. **15**, 6236 (2024).
[25] T. Chanda, S. Kaur, H. Singh, K. Watanabe, T. Taniguchi, M. Jain, U. Khanna, A. C. Balram, and A. Bid, Even denominator fractional quantum Hall states in the zeroth Landau level of monolayer-like band of ABA trilayer graphene, arXiv:2502.06245.
[26] J. Falson, D. Maryenko, B. Friess, D. Zhang, Y. Kozuka, A. Tsukazaki, J. H. Smet, and M. Kawasaki, Even-denominator fractional quantum Hall physics in ZnO, Nat. Phys. **11**, 347 (2015).
[27] Q. Shi, E.-M. Shih, M. V. Gustafsson, D. A. Rhodes, B. Kim, K. Watanabe, T. Taniguchi, Z. Papić, J. Hone, and C. R. Dean, Odd- and even-denominator fractional quantum Hall states in monolayer WSe_2, Nat. Nanotechnol. **15**, 569 (2020).
[28] M. Banerjee, M. Heiblum, V. Umansky, D. E. Feldman, Y. Oreg, and A. Stern, Observation of half-integer thermal Hall conductance, Nature (London) **559**, 205 (2018).
[29] B. Dutta, V. Umansky, M. Banerjee, and M. Heiblum, Isolated ballistic non-Abelian interface channel, Science **377**, 1198 (2022).
[30] A. K. Paul, P. Tiwari, R. Melcer, V. Umansky, and M. Heiblum, Topological thermal Hall conductance of even-denominator fractional states, Phys. Rev. Lett. **133**, 076601 (2024).
[31] R. A. Melcer, A. Gil, A. K. Paul, P. Tiwari, V. Umansky, M. Heiblum, Y. Oreg, A. Stern, and E. Berg, Heat conductance of the quantum Hall bulk, Nature (London) **625**, 489 (2024).
[32] A. Bid, N. Ofek, H. Inoue, M. Heiblum, C. L. Kane, V. Umansky, and D. Mahalu, Observation of neutral modes in the fractional quantum Hall regime, Nature (London) **466**, 585 (2010).
[33] B. Dutta, W. Yang, R. Melcer, H. K. Kundu, M. Heiblum, V. Umansky, Y. Oreg, A. Stern, and D. Mross, Distinguishing between non-Abelian topological orders in a quantum Hall system, Science **375**, 193 (2022).
[34] M. Yutushui, A. Stern, and D. F. Mross, Identifying the $\nu = \frac{5}{2}$ topological order through charge transport measurements, Phys. Rev. Lett. **128**, 016401 (2022).
[35] S. Manna, A. Das, M. Goldstein, and Y. Gefen, Full classification of transport on an equilibrated 5/2 edge via shot noise, Phys. Rev. Lett. **132**, 136502 (2024).
[36] J. Park, C. Spånslätt, and A. D. Mirlin, Fingerprints of anti-Pfaffian topological order in quantum point contact transport, Phys. Rev. Lett. **132**, 256601 (2024).
[37] M. Yutushui and D. F. Mross, Identifying non-Abelian anyons with upstream noise, Phys. Rev. B **108**, L241102 (2023).
[38] M. Yutushui, A. Stern, and D. F. Mross, Universal charge conductance at Abelian–non-Abelian quantum Hall interfaces, Phys. Rev. Lett. **134**, 206301 (2025).
[39] S. H. Simon, Interpretation of thermal conductance of the $\nu =$ 5/2 edge, Phys. Rev. B **97**, 121406(R) (2018).
[40] D. E. Feldman, Comment on "Interpretation of thermal conductance of the $\nu = 5/2$ edge", Phys. Rev. B **98**, 167401 (2018).
[41] S. H. Simon, Reply to "Comment on 'Interpretation of thermal conductance of the $\nu = 5/2$ edge"', Phys. Rev. B **98**, 167402 (2018).
[42] K. K. W. Ma and D. E. Feldman, Partial equilibration of integer and fractional edge channels in the thermal quantum Hall effect, Phys. Rev. B **99**, 085309 (2019).
[43] S. H. Simon and B. Rosenow, Partial equilibration of the anti-Pfaffian edge due to Majorana disorder, Phys. Rev. Lett. **124**, 126801 (2020).
[44] H. Asasi and M. Mulligan, Partial equilibration of anti-Pfaffian edge modes at $\nu = 5/2$, Phys. Rev. B **102**, 205104 (2020).
[45] M. Levin and B. I. Halperin, Collective states of non-Abelian quasiparticles in a magnetic field, Phys. Rev. B **79**, 205301 (2009).
[46] S. K. Singh, C. Wang, C. T. Tai, C. S. Calhoun, K. A. Villegas Rosales, P. T. Madathil, A. Gupta, K. W. Baldwin, L. N. Pfeiffer, and M. Shayegan, Topological phase transition between Jain states and daughter states of the $\nu = 1/2$ fractional quantum Hall state, Nat. Phys. **20**, 1247 (2024).
[47] K. Huang, H. Fu, D. R. Hickey, N. Alem, X. Lin, K. Watanabe, T. Taniguchi, and J. Zhu, Valley isospin controlled fractional quantum Hall states in bilayer graphene, Phys. Rev. X **12**, 031019 (2022).
[48] R. Kumar, A. Haug, J. Kim, M. Yutushui, K. Khudiakov, V. Bhardwaj, A. Ilin, K. Watanabe, T. Taniguchi, D. F. Mross, and Y. Ronen, Quarter- and half-filled quantum Hall states and their competing interactions in bilayer graphene, Nat. Commun. **16** 7255 (2024).
[49] M. Yutushui, M. Hermanns, and D. F. Mross, Paired fermions in strong magnetic fields and daughters of even-denominator Hall plateaus, Phys. Rev. B **110**, 165402 (2024).
[50] E. Zheltonozhskii, A. Stern, and N. H. Lindner, Identifying the topological order of quantized half-filled Landau levels through their daughter states, Phys. Rev. B **110**, 245140 (2024).
[51] B. I. Halperin, P. A. Lee, and N. Read, Theory of the half-filled Landau level, Phys. Rev. B **47**, 7312 (1993).
[52] J. K. Jain, *Composite Fermions* (Cambridge University Press, Cambridge, UK, 2007).
[53] A. Wójs and J. J. Quinn, Three-body correlations and finite-size effects in Moore-Read states on a sphere, Phys. Rev. B **71**, 045324 (2005).
[54] H. Wang, D. N. Sheng, and F. D. M. Haldane, Particle-hole symmetry breaking and the $\nu = \frac{5}{2}$ fractional quantum Hall effect, Phys. Rev. B **80**, 241311 (2009).
[55] A. Wójs, C. Toke, and J. K. Jain, Landau-level mixing and the emergence of Pfaffian excitations for the 5/2 fractional quantum Hall effect, Phys. Rev. Lett. **105**, 096802 (2010).
[56] E. H. Rezayi and S. H. Simon, Breaking of particle-hole symmetry by Landau level mixing in the $\nu = 5/2$ quantized Hall state, Phys. Rev. Lett. **106**, 116801 (2011).
[57] K. Pakrouski, M. R. Peterson, T. Jolicoeur, V. W. Scarola, C. Nayak, and M. Troyer, Phase diagram of the $\nu = 5/2$ fractional quantum Hall effect: Effects of Landau-level mixing and nonzero width, Phys. Rev. X **5**, 021004 (2015).
[58] E. H. Rezayi, Landau level mixing and the ground state of the $\nu = 5/2$ quantum Hall effect, Phys. Rev. Lett. **119**, 026801 (2017).

[59] N. Read and D. Green, Paired states of fermions in two dimensions with breaking of parity and time-reversal symmetries and the fractional quantum Hall effect, Phys. Rev. B **61**, 10267 (2000).

[60] A. C. Balram, M. Barkeshli, and M. S. Rudner, Parton construction of a wave function in the anti-Pfaffian phase, Phys. Rev. B **98**, 035127 (2018).

[61] M. Yutushui and D. F. Mross, Large-scale simulations of particle-hole-symmetric Pfaffian trial wave functions, Phys. Rev. B **102**, 195153 (2020).

[62] A. C. Balram, S. Mukherjee, K. Park, M. Barkeshli, M. S. Rudner, and J. K. Jain, Fractional quantum Hall effect at $\nu = 2 + 6/13$: The parton paradigm for the second Landau level, Phys. Rev. Lett. **121**, 186601 (2018).

[63] X. G. Wen and A. Zee, Shift and spin vector: New topological quantum numbers for the Hall fluids, Phys. Rev. Lett. **69**, 953 (1992).

[64] T. H. Hansson, M. Hermanns, S. H. Simon, and S. F. Viefers, Quantum Hall physics: Hierarchies and conformal field theory techniques, Rev. Mod. Phys. **89**, 025005 (2017).

[65] M. Yutushui, M. Hermanns, and D. F. Mross, Non-Abelian phases from the condensation of Abelian anyons, Phys. Rev. Lett. **135**, 056501 (2025).

[66] B. A. Bernevig and N. Regnault, Anatomy of Abelian and non-Abelian fractional quantum Hall states, Phys. Rev. Lett. **103**, 206801 (2009).

[67] B. Hunt, J. Li, A. Zibrov, L. Wang, T. Taniguchi, K. Watanabe, J. Hone, C. Dean, M. Zaletel, R. Ashoori, *et al.*, Direct measurement of discrete valley and orbital quantum numbers in bilayer graphene, Nat. Commun. **8**, 948 (2017).

[68] A. Haug, R. Kumar, T. Firon, M. Yutushui, K. Watanabe, T. Taniguchi, D. F. Mross, and Y. Ronen, Interaction-driven quantum phase transitions between topological and crystalline orders of electrons, Phys. Rev. X **16**, 011039 (2026).

[69] Z. Papic, N. Regnault, G. Moeller, *et al.*, DiagHam (2026), https://www.nick-ux.org/diagham/index.php/Main_Page.

[70] F. C. Zhang and S. Das Sarma, Excitation gap in the fractional quantum Hall effect: Finite layer thickness corrections, Phys. Rev. B **33**, 2903 (1986).

[71] The re-emerging $L = 0$ states for (15, 30) near $\theta = \frac{\pi}{2}$ have negligible overlap (0.1%) with those at smaller θ. They likely describe a distinct phase from the Jain 3/7, but the filling and shift do not match any other topological order known to us.

[72] K. K. W. Ma, M. R. Peterson, V. W. Scarola, and K. Yang, Fractional quantum Hall effect at the filling factor $\nu = 5/2$, in *Encyclopedia of Condensed Matter Physics*, edited by T. Chakraborty, 2nd ed. (Academic Press, Oxford, 2024), pp. 324–365.

[73] A. C. Balram and N. Regnault, Fractional quantum Hall effect of partons and the nature of the 8/17 state in the zeroth Landau level of bilayer graphene, Phys. Rev. B **110**, L081114 (2024).

[74] M. R. Peterson, K. Park, and S. Das Sarma, Spontaneous particle-hole symmetry breaking in the $\nu = 5/2$ fractional quantum Hall effect, Phys. Rev. Lett. **101**, 156803 (2008).

[75] G. J. Sreejith, Y. Zhang, and J. K. Jain, Surprising robustness of particle-hole symmetry for composite-fermion liquids, Phys. Rev. B **96**, 125149 (2017).

[76] B. Kuśmierz, A. Wójs, and G. J. Sreejith, Mean-field approximations for short-range four-body interactions at $\nu = \frac{3}{5}$, Phys. Rev. B **99**, 235141 (2019).

[77] W. Hutzel, J. J. McCord, P. T. Raum, B. Stern, H. Wang, V. W. Scarola, and M. R. Peterson, Particle-hole-symmetric model for a paired fractional quantum Hall state in a half-filled Landau level, Phys. Rev. B **99**, 045126 (2019).

[78] M. Yutushui, A. Dey, and D. F. Mross, Data supplement for "The numerical case for identifying non-Abelian phases by their daughters", [Data set], Zenodo (2025), http://doi.org/10.5281/zenodo.16618924.

[79] R. V. Mishmash, D. F. Mross, J. Alicea, and O. I. Motrunich, Numerical exploration of trial wave functions for the particle-hole-symmetric Pfaffian, Phys. Rev. B **98**, 081107 (2018).

[80] R. E. Wooten, Haldane pseudopotentials and Landau level mixing in the quantum Hall effect, Ph.D. thesis, University of Tennessee, 2013.

[81] M. Yutushui and D. F. Mross, Phase diagram of compressible and paired states in the quarter-filled Landau level, Phys. Rev. B **111**, 035106 (2025).

[82] A. C. Balram, Transitions from Abelian composite fermion to non-Abelian parton fractional quantum Hall states in the zeroth Landau level of bilayer graphene, Phys. Rev. B **105**, L121406 (2022).

[83] A. Sharma, S. Pu, A. C. Balram, and J. K. Jain, Fractional quantum Hall effect with unconventional pairing in monolayer graphene, Phys. Rev. Lett. **130**, 126201 (2023).